IITRI–SMRI Solution Mining Studies

Richard H. Snow
Hugo J. Nielsen
IIT Research Institute
Technology Center
Chicago, Illinois 60616

ABSTRACT

A model of the solution processes in a solution mine cavity was developed based on boundary layer theory. Computer predictions of solution rates were compared with data from laboratory experiments on perfect salt crystals, and a discrepancy of a factor of 3 resulted. The discrepancy was traced to inadequacy of the Colburn j-factor correlation for predicting the mass transfer coefficient at the high Schmidt number (1000) of salt in water. Reasonable results were obtained when the j-factor was changed to depend on the Schmidt number to the 0.52 power, a value that is in agreement with the penetration theory.

The model includes different thickness parameters for the profiles of concentration and velocity in the boundary layer, and this is necessary to predict correct brine production rates. Experimental techniques to measure these profiles were developed; preliminary results indicate that the ratio of the thickness is 0.03 for salt in water.

A computer program was developed to predict the cavity growth and shape, the build-up of a concentration pattern in the bulk solution and its effect on the boundary layer, and the concentration of brine produced over a period of time when the feed water is top injected. The analysis can be extended to other cases.

PROBLEM DEFINITION

The objective of this project is to understand the processes that govern the solution of salt in a solution mine. The problem is important to the member companies of the Solution Mining Research Institute because this knowledge can determine the conditions which lead to the most efficient production of brine. This includes developing a cavity of a shape that minimizes the tendency of roof falls, which can end production of a brine well altogether. Another objective is the prediction of the dimensions of the cavity, which determine the location of potential ground subsidence. This information is important from the point of view of property losses, especially since there is still no adequate means of measuring the size and shape of an underground cavity, at least in the presence of irregular wall shapes, piles of fallen rock, and uncertain configurations near the casing seal.

A computer program was written from available boundary layer theory to predict the rate of cavity growth. However, laboratory experiments on small salt samples showed that the predictions were in error by a factor of 3. This was surprising, since boundary layer theory gives accurate results for mass transfer of other materials. On further study, it was found that the properties of salt are rather unusual, in that it has a Schmidt number of about 1000, while most materials that have been studied have a smaller Schmidt number. Consequently, some of the equations were not valid when applied to salt.

As a result, it was decided that further measurements of velocity and concentration profiles in the salt boundary layer were necessary. Techniques to make these measurements had to be developed, since such measurements have never been done for a material with the properties of salt. A digression in the original research plan was, therefore, necessary, and this phase of the work is only now

coming to fruition. In the meantime an empirical modification in the mass-transfer equation has been made, and it is believed that the computer model now gives valid results.

LITERATURE STUDY

A study of the literature revealed only one direct observation of the shape of a full-scale cavity by Trump (1947). Some experiments on dissolving of cavities in blocks of salt had been done at the University of Texas, (Leont'ev, and Kidryaskin, 1966). These gave indications of the type of convective flow to be expected, but there was no assurance that different behavior would not occur when scaled up 100-fold to an actual mine cavity size.

Further experiments by Durie (1963) at the University of Texas on slabs of rock salt indicated that the convective flow of a boundary layer near the salt face is the most important phenomenon in determining the solution process. Durie also investigated the boundary layer theory. He applied the equations of Eckert and Jackson (1951) developed for forced convection heat transfer in pipes, to the free convection salt solution process. Although Durie's results did not fully agree with experiment, we concluded that this approach was worth investigating further, because the boundary layer behavior appeared to be the main process determining the solution rate and cavity growth.

Although there is an extensive literature on boundary layer theory, most of it is not directly applicable to the salt solution problem. For example, many articles present experimental results on rates of mass or heat transfer in terms of empirical dimensionless equations that are valid only for special conditions, but not for the conditions of salt dissolving. A long-range plan was prepared, beginning with further development of the boundary layer theory in the first year, and extending to other important effects in subsequent years.

BASIC PHENOMENA AFFECTING SOLUTION IN A CAVITY

At this point it is worthwhile to summarize the important effects occurring in the cavity.

The rate of solution of a material such as salt is determined primarily by the conditions in the fluid. Conditions in the solid are important too, but their effects are superimposed on the fluid behavior. If the solid is a perfect crystal, only one property of the solid is of primary importance: the solubility. Two other variables of imperfect salt may be important: the fraction of its surface that is covered by impurities and the roughness of its surface.

An important property of the fluid is the diffusivity of the salt molecules in solution. Since solution cannot take place when saturated brine is adjacent to the crystal face, diffusivity allows solution to occur by transporting salt molecules away from the face. An analysis of published salt diffusivity data showed that previous workers used an inconsistent definition of diffusivity that led to a 25% error in some cases.

A second property of the fluid that affects solution rate is the flow behavior. Flow aids the removal of dissolved salt from the crystal face.

Fluid flow may arise from two sources: forced convection, caused, for example, by pumping into the cavity; and free convection, caused by density differences. If both occur at once, the situation is difficult to analyze. However, calculations showed that the flow velocity due to pumping is important only during the first hours of cavity operation. After that, flow due to pumping can cause mixing of the bulk fluid in the cavity if there is bottom injection, but forced flow does not normally reach the salt face directly.

Free, or natural convection is the most important phenomenon in the cavity. It is caused by the increased density of concentrated brine near the salt face compared with the density of brine in the bulk of the cavity. The downward flow of dense brine, and simultaneous molecular diffusion govern the concentration profile adjacent to the salt face and determine the rate of solution. Flow, in turn, is limited by drag of the fluid against the salt face and drag against the bulk fluid. Thus a balance of forces determines the velocity profile against the salt face. If the flow increases to the point where it becomes turbulent, this causes additional mixing which in turn affects the concentration profile and the solution rate.

DEVELOPMENT OF BOUNDARY LAYER THEORY

The general differential equations for boundary layers are known (Eckert and Jackson, 1951). If these equations could be solved exactly to determine the flow pattern throughout the boundary layer at any depth in the cavity, then the solution rate would also be determined. In general, these equations can only be solved on a computer. Even then, the problem is too difficult to obtain a practical answer in a reasonable time with the largest

computer. The reason is that the equations would have to be numerically integrated first along a direction normal to the salt face, then along the depth of the cavity, and then over time.

Eckert and Jackson (1951) solved a similar problem for the case of forced convection heat transfer in a pipe by assuming that the velocity and temperature profiles across the thickness of the boundary layer can be expressed by certain power functions. This made it possible to evaluate the integrals of the flow equations once, and thus reduce the complexity of the problem by an order of magnitude. In fact, for laminar flow, they were also able to integrate the equations explicitly along the length of the face, so that a computer was not needed. For turbulent flow, the integration could be done only when the bulk fluid had constant temperature. Several other assumptions were also made.

In their approach, an empirical element is introduced in the form of the boundary layer profiles, as well as the relation of shear stress at the wall to N_{Re}.

Durie (1963) applied the formulation of Eckert and Jackson (1951) to the problem of salt solution in a boundary layer. Durie used Eckert's method of integrating the boundary layer equations, which is limited to the case where the flow is laminar and the bulk concentration is constant throughout the cavity. These assumptions are not valid in an actual mine cavity. In addition, Durie's predicted results differed from his experimental results and he found it necessary to apply an empirical correction of about a factor of 2. The reasons for the discrepancy were not clear, and there was no way to know whether the discrepancy would increase as the scale of the experiments was increased from 1-ft samples to an actual cavity hundreds of feet in size.

The boundary layer theory of Eckert and Jackson is strictly valid only when the profiles of velocity and concentration are the same, which is true when the Schmidt number $N_{sc} = 1$. This is true in heat transfer, but in salt solution, it is far from true. During the first year of the project, we modified the theory by introducing another empirical parameter λ into the boundary layer integrals. This parameter is the ratio of the thickness of the concentration boundary layer to the thickness of the velocity boundary layer. This modification correctly represented these integrals for N_{sc} different from 1.

The new formulation recognized that when the two boundary layer profiles are different, mass and momentum are not transferred at the same rate. Physically, this means that a thin layer of dense brine flows down very close to the salt face. The viscosity of water is large enough so that this dense brine can drag down a relatively thick layer of bulk fluid whose density has not been altered much. Although Durie recognized this, his equations did not. It is important to correctly represent this effect, because it determines the amount of flow down the mine cavity wall. This, in turn, determines the circulation of brine in the cavity, and the amount and concentration of brine that can be produced.

In a solution mine cavity there is an additional effect that was not present in previous studies of convection. This is the effect of removal of brine by well operation and its replacement by fresh water. As a result of the history of withdrawal of brine from a particular cavity during its growth, the concentration pattern in the bulk of the cavity may take any arbitrary form. Therefore, the solution mine model was designed to take into account an arbitrary stratification pattern of the bulk fluid.

Not only does well operation change the fluid present in the cavity, but it also causes mixing. However, mixing is minimized in the case of reverse operation, where brine is removed from the bottom of the cavity and fresh water is injected at the top, since the fresh water tends to lie on the more dense brine and not mix. This effect was observed even in small laboratory cavities in salt at University of Texas. We have done most of our calculations for this simpler case.

The case of normal injection can also be described mathematically. Fresh water rises when introduced at some point in the cavity due to its buoyancy with respect to the surrounding brine. A jet forms in which the amount of entrained brine can be calculated. Mixing due to entrainment in the rising jet can be predicted, as well as conditions which will maintain the fluid at a uniform concentration above the point at which the water is introduced. The mine model was modified to include operation under these conditions.

EXPERIMENTS ON SOLUTION OF SALT

The only previously reported measurements on convective solution of salt slabs were those done at the University of Texas. It was difficult to interpret these experiments because it was not possible to separate the effects on the solution rate of salt imperfections from effects of the boundary layer. Two effects of imperfections were observed, however: increased solution rate below an insoluble layer, and pitting.

Our experiments were aimed at separating the effects of imperfections and of the boundary layer flow. Some understanding was gained by experiments on solution of natural crystals from the International Mine. These were near-perfect crystals, but they contained some small bubbles. It was observed that the solution of such crystals was initially uniform and followed the predictions of the boundary layer theory, but eventually pitting developed at each bubble that became exposed to the solution process. These pits were found to eat their way into the salt much faster than the rate of solution at a smooth face. Experiments were next done on sawed pieces of rock salt from the International Mine. These dissolve initially at nearly the same rate as a perfect crystal, but the rate increases over a period of hours by as much as a factor of 5. (Durie made similar measurements on rock salt). We observed that pitting occurs with rock salt similar to that with bubble crystals, and we believe that a similar mechanism operates. In the case of rock salt, a pit may be originated by additional types of imperfections such as insoluble inclusions and cracks caused by relief of stress when the sample is taken from the ground.

Allen McCue told us of experiments done at FMC Corporation of solution of optical salt crystals that did not produce any pitting. We obtained some optically perfect crystals from Harshaw Chemical Company and confirmed this experimental result. We also obtained similar results with bubble-free natural crystals from the Fairport Mine of Morton Salt Company. In addition, we found that minute defects in the crystal do not affect the solution process as long as the imperfections are much smaller than the thickness of the boundary layer. For example, scratches made by 400-mesh grit are removed by the solution process.

Solution of Near-Perfect Salt.

Figure 1 gives results for solution of a vertical face of near-perfect salt in brine of various concentrations as a function of depth from the top of the sample. A (100) crystal face, or cube face, was dissolved in each case, except for two indicated experiments where a (110) (face diagonal) or (111) (cube diagonal) face was specially polished and dissolved. The solution rate was somewhat less on the diagonal faces, which concurs with the fact that the solubility is less on such faces.

The solution rate is greatest at the top of the sample, where the boundary layer is thin. The solution rate decreases to very low values at high bulk concentrations. These data span the region in

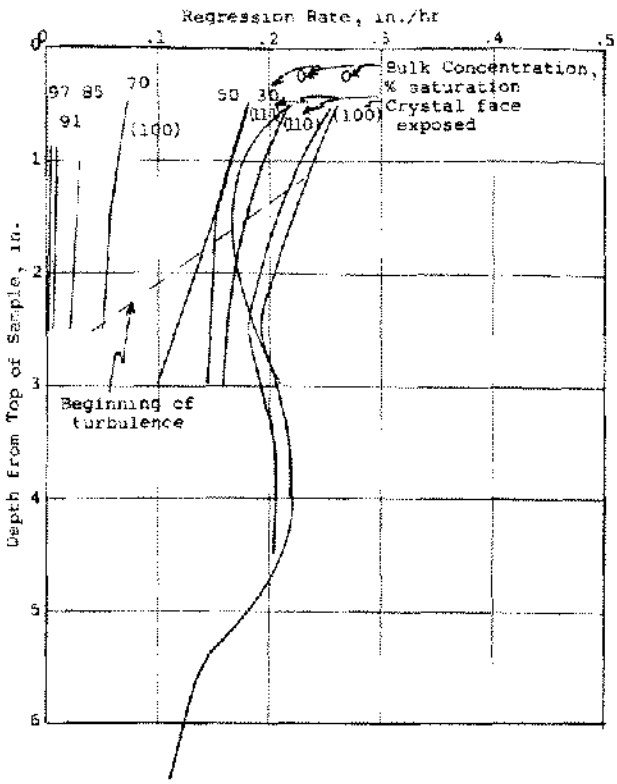

Figure 1. Rates of regression of near-perfect single salt crystals oriented vertically in water and brine.

which the flow of the boundary layer undergoes transition from laminar to turbulent, except for bulk concentrations above 85% saturation, where the flow was laminary to the bottom of the sample. The depth of transition of flow is shown by a dashed line in Figure 1. Note that the regression rate decreases in going down the salt face in the laminar regime. At the transition to turbulence, the regression rate increases for some distance and then decreases again.

One experiment was done with a crystal in the horizontal position, with the exposed salt face as a roof. The regression was uniform over the whole surface. The surface was irregularly covered with fine 1/16-in. pits, apparently marking convection cells. These pits did not grow in diameter, as do pits in a vertical face due to imperfections.

The important conclusion was that these experimental results should be comparable with the results of the boundary layer theory. It then became possible to check the validity of the assumptions made in deriving the boundary layer theory by comparing the calculated results with experiments on perfect salt.

Solution of Massive Salt.

Results of experiments with massive salt slabs from the International Mine are presented in Table 1 and Figure 2.

The rate of solution of smoothed samples of rock salt when first put into water is similar to that of perfect salt crystals. As solution progresses, however, the imperfect salt develops increasing roughness, and this causes the solution rate to increase. The origin of each detail of roughness may be an air bubble, a grain of insoluble material, a boundary between adjacent crystals with different orientation, a crack, or an insoluble layer. Once a recess starts to form at an isolated point, it makes little difference what the source of the imperfection was. Apparently an eddy or circulation of fluid can be set up in a recess, causing a high rate of solution there. As a result of this the solution rate of imperfect salt increases with time as these recesses grow.

Table 1 shows that the regression rate is relatively large in the top 2 in. but shows no trend from there down to 15 in. The surface is marked with pocks or recesses 1/2 to 1 in. diameter and 1 to 2 in. in depth. In addition some cracks (produced when the sample was removed from the mine) serve as channels for flow in brine. These cracks rapidly widen and increase the average weight regression rate of the sample. The cracks extend to the back of the sample, 4 in. Such flow through cracks is usually stopped by a horizontal rock layer. (Not all cracks develop in this way;

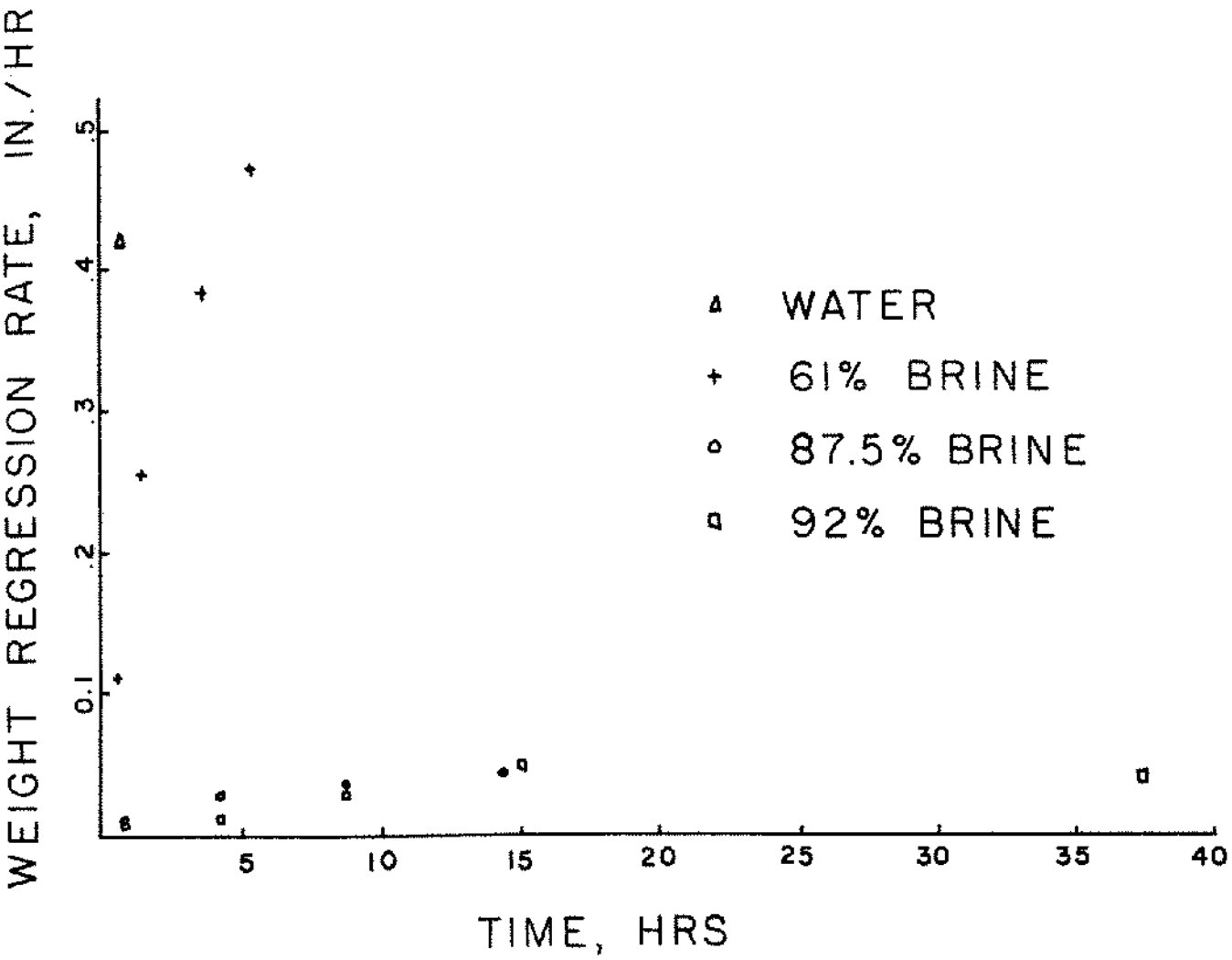

Figure 2. Rates of regression of massive salt versus time.

TABLE 1. Solution of Large Massive Salt from International Mine at Comparable Extent of Solution

Sample	Bulk Concentration, % saturation	Depth of Measurement, in.	Regression Rate, in./hr. Caliper	Regression Rate, in./hr. Weight	Probe Concentration 0.004 in. from Wall, $Y - Y_f/Y_s - Y_f$	Transition Depth, in.
5-17 (at 1/2 hr)	0	0.5	0.62			1-2
		2	0.51			
		4	0.28			
		6	0.36			
		8	0.31		21	
		11	0.51			
		13	0.34			
		15	0.39			
			Mean 0.46	1.36		
5-18 (at 1/2 hr)	0	4	0.47			
		5	0.41			
		7	0.49			
		9	0.45		5.3	
		11	0.41			
		13	0.47		2.2	
		15	0.42			
			Mean 0.44	0.43		
5-19 (Roof position) (at 1/2 hr)	0		0.94			
			0.62			
			0.88			
			0.86			
			0.64			
			0.76			
			Mean 0.78	1.15		
				1.4 (at 1 1/2 hr)		
6-6 (at 2 1/2 hr)	61	1	0.10			
		4	0.15			
		7	0.18			
		10	0.16			
		12	0.20			
			Mean 0.17	0.45		
10-7 (at 8 hrs)	85.7	1	0.024			
		4	0.018			
		7	0.020			
		10	0.020			
			Mean 0.020	0.030		
9-25 (at 15 hrs)	93.5	1	0.039			
		4	0.025			
		7	0.023			
		10	0.023			
		14	0.024			
			Mean 0.023	0.041		

partial-cleavage cracks in single crystals do not grow, probably because these cracks are initially too thin for fluid to flow in them.) The driving force for such flow is the greater density of brine in a crack caused by solution.

Rough undulations are observed in the surface of massive salt that has been partially dissolved. Perhaps loose grains of salt can start the development of a pit-hole recess. Flakes of insoluble impurities such as anhydrite falling down with the boundary layer flow can be seen. There is no evidence that these insoluble impurities adhere to the surface and prevent solution with this particular type of salt. Some paper-thin layers of anhydrite protrude from the surface, stir the boundary layer, and cause increased solution at a point below the protrusion. This may be a main cause of pitting in such salt.

In these experiments, the regression rate just below a rock layer was twice that above the layer. This effect was also observed by Durie (1963). Apparently, the projecting rock layer causes the boundary layer to mix, so that the salt just below the layer is exposed to weaker brine and dissolves at a rate more like the rate at the top of the salt sample itself.

The first massive salt sample (5-17) was oriented with its cut face vertical and the remaining faces covered with plasticene. The bedding plane of the salt was in its normal orientation. The second sample (5-18) face was also in a vertical plane, but it had been cut at a 30° angle to the bedding plane. The boundary layer flow moved directly downward, even over obstacles. Differences in the regression rates of different samples at the same conditions are probably due to differences in the imperfections and cracks in the surface that happens to be exposed.

The third slab (5-19) was dissolved in a position as if it were the roof of a cavity and was cut in a direction such that the bedding plane was also in its normal orientation. The regression rate of this sample was not much different from that of the vertical samples. The surface was rough, but large cracks did not open up in the salt.

Sample 6-6 was, again, in normal vertical position, but the bulk concentration was 61% saturation. Caliper regression rates are averaged for the first 2 1/2 hrs and ignore deep crevices and pits that formed.

Sample 10-7 was dissolved in brine of 85.7% saturation, while sample 9-25 was dissolved in brine of 93.5% saturation. For these experiments the variation of caliper regression rate with concentration approximately followed the law

$$dR/dt = K_c \rho_{salt} \Delta Y/(1-Y_0)$$

where the mass transfer coefficient K_C is practically independent of bulk concentration. The experiments confirmed the validity of this equation, which was used in the computer model.

These effects appear too complicated to permit a purely theoretical prediction of the solution rate of imperfect salt at the present time. Instead, we propose to modify the model for perfect salt so that it fits the experimental results for imperfect salt. If this is done correctly, it is likely that the resulting semi-empirical model will give correct results for a wider range of conditions than those under which the experimental corrections were determined. For example, it should be possible to determine experimental factors from solution of core samples and to predict cavity growth for a particular salt with the boundary-layer model.

MODIFICATION OF BOUNDARY THEORY AND COMPARISON WITH EXPERIMENT

The computer program for cavity growth calculations could also be used to predict the rate of solution of salt crystals in the laboratory, and comparison with experimental results for perfect crystals provided a check of the theory. The results did not agree. A thorough study of the boundary layer theory and its assumptions was done before the cause of the discrepancy was found.

The experimental results for perfect salt crystals in Figure 1 showed, for example, that at a depth of 4.5 in. from the top of a salt crystal in pure water the regression rate is 0.21 in/hr. The results of the computer calculations depend on the value chosen for the parameter λ, which is the ratio of the thickness of the concentration boundary layer to that of the velocity boundary layer. Preliminary measurements of the variation of concentration and velocity across these boundary layers indicated that the value of λ is near 0.03, and this agrees with a theoretical estimate based on the value of $N_{sc} = 1000$ for salt solution. A computer calculation with this value of λ predicts a solution rate of only 0.09, which is a factor of 2.2 lower than the experimental result.

The main cause of the discrepancy was found to lie in the use of the Colburn j-factor relation. This equation relates the mass transfer coefficient to the

shear stress at the salt surface. It is based on the "analogy theory," which is known to be valid for forced convection experiments if $N_{sc} = 1$. The equation also contained an empirical correction factor equal to $N_{sc}^{2/3}$. This factor is based on the classical work of Colburn; however, the data available to Colburn extended only to $N_{sc} = 10$. Jakob (1949) reported heat transfer results up to a Pradtl number (or Schmidt number) of 75, and he found that the exponent is 0.58. Also, the penetration theory of mass transfer (Treybal, 1968) predicts that the exponent is 0.5.

The Schmidt number dependence may be considered an unknown function, and a value may be fitted to agree with our experiments. This procedure resulted in an exponent of 0.52. We used this value in subsequent calculations.

A more direct experimental determination of the profiles of the velocity and concentration boundary layers would give a better value of λ for use in the calculations. A different value of λ would require a different value of the exponent to fit experimental solution rates.

A number of other checks were made of the theory and computer program. Calculations were done for constant bulk concentration to compare with the analytical solution of Eckert and Jackson for this case. The results agreed. This was primarily a check of the accuracy of the computer programming.

Wasan (1967) suggested that injection of the mass of salt dissolved into the boundary layer can affect the velocity profile due to the horizontal component of velocity of the salt. A trial calculation indicated that this effect results in, at most, a 10% correction.

Another assumption underlying the theory is that λ remains constant with increasing depth down the wall of the cavity. There is no evidence on this point for free convection, and this is another reason for measuring the actual profiles.

COMPUTER CALCULATIONS OF CAVITY GROWTH RATES

A series of computer calculations was done to determine whether the model predicts reasonable solution behavior, to compare the predictions with laboratory experiments, to investigate the effect of certain parameters in the model, and to predict the duration of the proposed cavity experiment in the International Mine. Only one example is presented here, Figure 3. This figure shows the computer outline of the cavity at various stages of development.

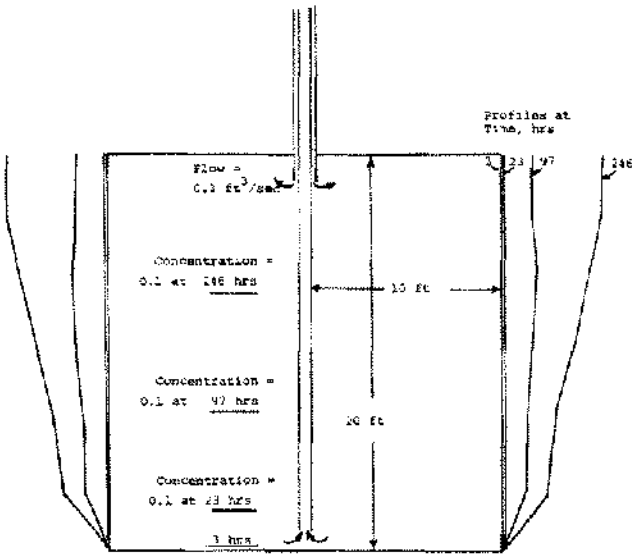

Figure 3. Calculated growth of cavity wall and buildup of bulk concentration.

It also indicates the computer position of a halocline, or the height reached by accumulated brine of a concentration 0.10 weight fraction. This accumulation of brine is determined by the feed rate and the rate of convective flow down the cavity walls.

MEASUREMENT OF BOUNDARY LAYER CONCENTRATION PROFILES

A major effort has been devoted to developing a laser technique for measuring profiles of concentration across the thickness of the boundary layer. The measurement is difficult because the boundary layer is only about 10 mils thick on salt samples that can be measured in the laboratory. Such profiles have not been measured for free convection mass transfer, although measurements have been done for heat transfer.

An optical method has the most promise because it need not disturb the flow. An optical method can measure concentration because index of refraction is directly proportional to concentration. A difficulty of optical methods is that a beam of light must pass close to the salt surface within the boundary layer. The thinness of the boundary layer makes this difficult.

Several techniques using a laser beam as a source of collimated light were attempted. It was found that such a beam could be made to graze a

cylindrical salt surface and be bent toward the salt by the gradient of refractive index in the boundary layer. Some measurements were done by this method, but it was found to be limited to conditions near the top of a salt sample, where the boundary layer flow is laminar. Turbulent eddies distort the laser beam and prevent meaningful measurements.

Another technique was devised in which a laser beam enters through the back of the transparent salt crystal and emerges into the boundary layer. Since the beam is bent by the boundary layer, it can be made to reenter the salt crystal by proper choice of the angle of the laser beam with respect to the salt. This effect was observed experimentally. The beam was observed after passing through the boundary layer and the salt; undulations in the beam caused by eddies in the boundary layer were found to depend on the depth of penetration into the turbulent outer portion of the boundary layer.

The difficulty with these experiments was to find some property to measure from which the concentration gradient could be back-calculated. The following variables were considered, but were found to be too insensitive: critical angle at which the ray is bent back enough to reenter the salt, distance travelled along the salt before reentering, deflection of the ray from the angle of total reflection from the salt face. Recently it has been found that the distance the ray penetrates the boundary layer can be measured by introducing a 1-mil wire probe into the laser path with a micrometer drive as shown in Figure 4. By viewing the probe with a microscope focused through the salt sample, it is possible to determine when the probe enters the laser beam and becomes illuminated. The trajectory of the laser beam can then be determined from measurements of the distance from the edge of the beam and the salt face, using the same probe. Experimental trajectories determined by this means are given in Figures 5 to 7.

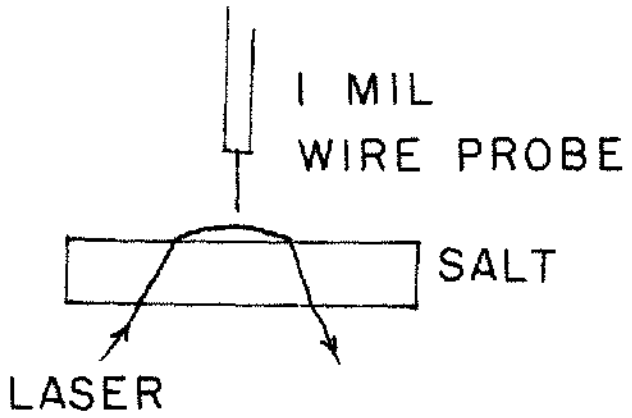

Figure 4. Geometry of wire probe to expose laser trajectory.

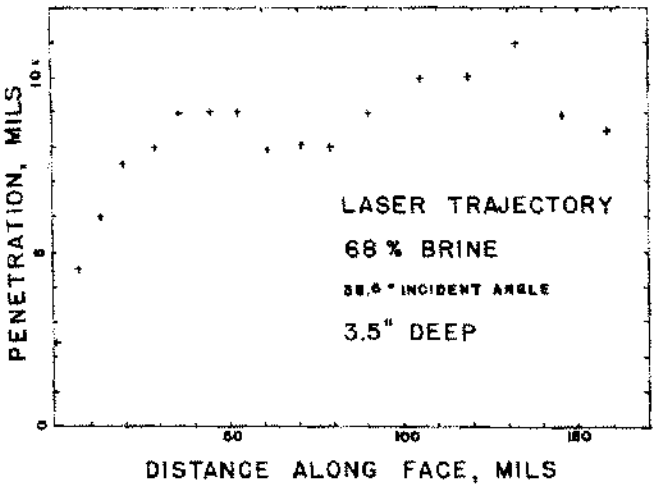

Figure 5. Laser trajectory, 68% brine, 3.5" deep.

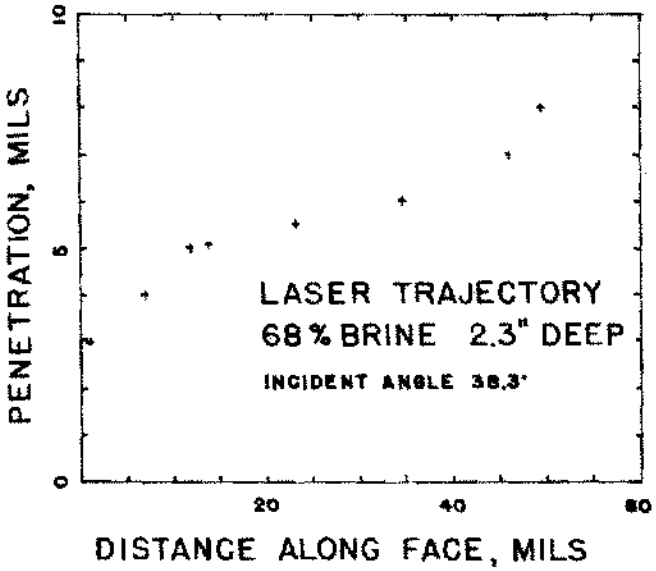

Figure 6. Laser trajectory, 68% brine, 2.3" deep.

In order to determine the concentration gradient from these measurements, a method of calculating laser ray trajectories was needed. A differential equation for the ray trajectory was derived, based on the statement in the literature that the bending

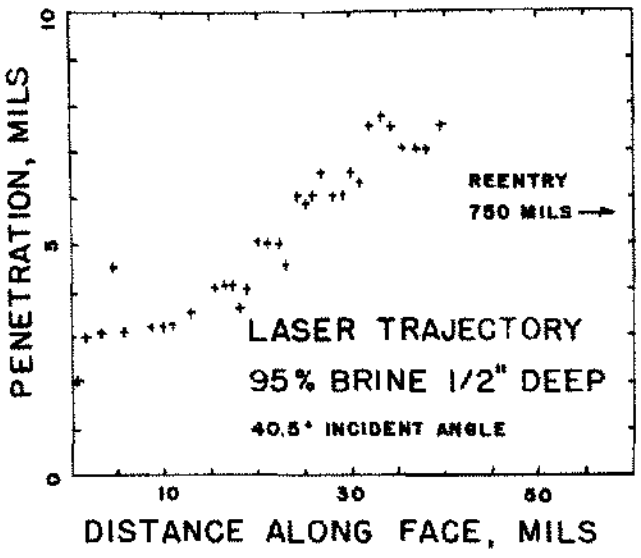

Figure 7. Laser trajectory, 95% brine, 1/2" deep.

of the ray (expressed as its curvature) is determined by the gradient of refractive index of the medium in a direction normal to the ray. This differential equation was solved on a computer for assumed boundary layer concentration profiles. Some conclusions have already been reached about the nature of the profiles as a result of these calculations. Neither the 1/7th—nor the 1/4th-power profiles are strictly valid, since they have a discontinuity of the first derivative of salt concentration at a distance δ from the salt face, and since the concentration gradient becomes infinite at the salt face. A modified form of profile was found that behaves properly in these respects, and yet does not differ much in other respects.

Table 2 lists numerical values of concentrations based on several assumed concentration-profile functions. In the table δ is a parameter called the boundary layer thickness, and n is the distance normal to the salt face. By performing a number of calculations of the ray trajectory it is possible to find a profile function that fits the experimental ray trace.

Some information about the nature of the concentration profile in the boundary layer was obtained from theoretical calculations of ray trajectories. In the studies with cylindrical salt samples it was noted that a concentration profile must have a continuous gradient at every point. If the gradient changes suddenly, the light ray equation cannot be integrated past this point. Physically there is no reason for such a discontinuity; it simply means that the usual 1/7th-power profile is incorrect in this respect. Physically the concentration could not have an infinite gradient at the surface so long as the fluid has a finite viscosity, which any real fluid must have. This defect has been noted by others in studies of the effect of roughness on the boundary layer. Mathematically they avoided the problem by translating coordinates so that the salt interface was located at a slight distance from y = O; in other words, the discontinuity was translated into

TABLE 2. Concentration-Profile Functions

$\frac{n}{\delta}$	$\exp\left[-2\left(\frac{n}{\delta}\right)\cdot\left(\frac{n}{\delta}\right)^{0.2}\right]$	$\exp\left[-2\left(\frac{n}{\delta}\right)\cdot\left(\frac{n}{\delta}\right)^{0.1}\right]$	$1-\left(\frac{n}{\delta}\right)^{1/7}$	$1-\left(\frac{n}{\delta}\right)^{1/4}$
10.00000	.000000	.000000		
5.00000	.000011	.000014		
2.00000	.005800	.006271		
1.00000	.049787	.049787	0.	0.
.50000	.154038	.144708	.094276	.159103
.20000	.324724	.286121	.205402	.331259
.10000	.435632	.369971	.280314	.437658
.05000	.522421	.431221	.348163	.527129
.02000	.008167	.488584	.428139	.623939
.01000	.658291	.521546	.482052	.683772
.00500	.700071	.549523	.530882	.734085
.00200	.746305	.582073	.588440	.788525
.00100	.776321	.604000	.627240	.822172
.00050	.802781	.025862	.662383	.850465
.00020	.833220	.652410	.703806	.881079

the salt crystal by adding a distance ϵ to n in the formulas of Table 1. The distance of translation ϵ becomes another parameter in the boundary layer profile equation, and it should be determined by experiments. This parameter should be very important for our work, since it defines the concentration gradient at the wall, which in turn determines the mass-transfer coefficient and the solution rate.

Calculation of Light Ray Trajectory

Tong (1967) states that the deflection of a beam in a medium of varying refractive index is such that the radius of curvature η depends inversely on the gradient of the index of refraction, N:

$$1/\eta = \text{grad } N \qquad (1)$$

In cartesian coordinates the radius of curvature is:

$$\eta = \frac{\left[1 + (y')^2\right]^{3/2}}{\pm y''} \qquad (2)$$

where a prime denotes differentiation with respect to y.

The gradient $\frac{\partial N}{\partial r}$ in a direction normal to the salt face is known from the assumed concentration profile. The refractive index is a linear function of concentration:

$$N = 1.333 + 0.179\,Y \qquad (3)$$

For example, if the concentration profile is

$$Y/Y_0 = \exp\left[-2\left(\frac{Y}{\delta}\right)\cdot\left(\frac{Y}{\delta}\right)^{0.1}\right] \qquad (4)$$

then

$$\text{Grad } N = -\frac{0.0471}{\delta}\left[2 + 0.1\left(\frac{Y}{\delta}\right)^{-0.9}\right]\exp\left[-2\left(\frac{Y}{\delta}\right)\cdot\left(\frac{Y}{\delta}\right)^{0.1}\right] \qquad (5)$$

where

δ is the boundary-layer thickness

Y is salt concentration

Y_0 is saturated salt concentration

Y is distance (in.) from salt face

N is refractive index of salt solution

η is radius of curvature of light-ray trajectory.

In a salt boundary layer the concentration is high at the salt face and drops off in the direction of the bulk solution. Therefore, a ray grazing the salt face is directed normal to the concentration gradient, and it is bent toward the salt face. If the ray is at an angle to the salt face, the gradient normal to the ray is $\frac{\partial N}{\partial r}\cos\varphi$ where φ is the angle between the ray and the salt surface. The basic equation is then:

$$\eta = \frac{\left[1 + (y')^2\right]^{3/2}}{y''} = \frac{1}{(\cos\varphi)\ (\text{Grad } N)} \qquad (6)$$

Since

$$\cos\varphi = \sqrt{1 + (y')^2}$$

Equation 1 can be solved for y", the second derivative of the ray trajectory:

$$y'' = -\frac{0.0471}{\delta}\left[1 + (y')^2\right]\left[2 + 0.1\left(\frac{Y}{\delta}\right)^{-0.9}\right]\exp\left[-2\left(\frac{Y}{\delta}\right)\cdot\left(\frac{Y}{\delta}\right)^{0.1}\right] \qquad (7)$$

Trajectories of some rays emerging from flat salt were computed. One trajectory is plotted in Figure 8. A calculation consists of following the path of a light ray. The initial condition for the calculation is a point and an assumed initial direction of the ray. The initial point was 10^{-6} in. from the salt surface in the boundary layer; in other words, the translation parameter was set equal to 10^{-6} in.

A second set of trajectories was calculated by a different method. A trajectory at an angle near critical was back-calculated by starting at a point well out into the bulk solution with a ray making a small angle, e.g., 1° to the salt face. The ray's slope is computed as it is traced back to the salt face. Thus, in one calculation the slopes are obtained at various distances from the face that correspond to

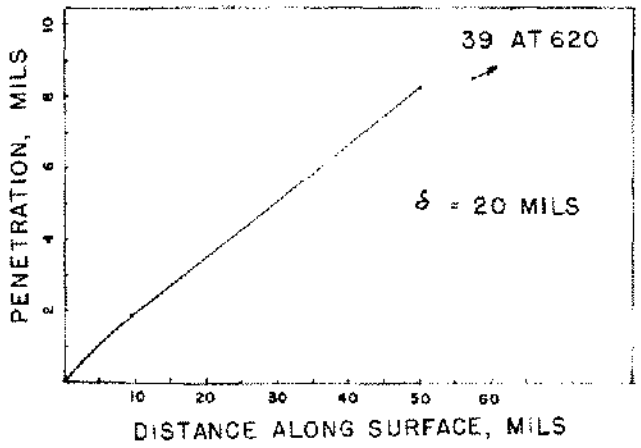

Figure 8. Calculated trajectory of laser just escaping.

various possible values of the translation parameter. The results are given in Table 3.

Trajectories were calculated for several values of the emerging angle. For a boundary layer thickness of $\delta = 0.5$ in., a calculation showed that the ray escapes from the boundary layer if the emerging angle is 15°, while it curves strongly downward and reenters the salt if its emerging angle is 10°. Experimentally the critical angle was formed to be about 12°.

Further experimental measurements are needed to obtain the variation of boundary layer parameters with depth and bulk concentration. Ray trace calculations have not yet been done for the exact conditions of these experiments, and values of the parameters have not yet been determined.

MEASUREMENT OF BOUNDARY LAYER VELOCITY PROFILES

One method of measuring velocity profiles is to observe the motion of particles in the flowing boundary layer as they pass through the laser beam in the experiment described above. Particles of 1 micron size can readily be seen, and their time of passage can be measured with a photomultiplier. Measurement of their depth in the boundary layer depends on observing them through a microscope with thin depth of field. Some preliminary measurements have shown that velocities can be measured between the salt surface and the velocity maximum.

Another method is a modification of a technique reported by Papovitch and Hummel (1967). It involves forming a line of dye normal to the salt surface by a flash photolysis technique, and then taking a motion picture of the line. Some pictures have been taken at 400 frames/sec. Velocities have been measured from the point of maximum velocity out into the bulk solution.

TABLE 3. Back-Calculation of Laser Traces That Just Escape from the Boundary Layer

δ, in.	Distance along Salt, in. x	Penetration into B.L., in. y	y′	y″	Angle
0.05	1.019	8.04×10^{-2}	-.032	- .032	
	.463	5.08×10^{-2}	-.065	- .095	
	.136	2.17×10^{-2}	.124	- .352	
	.0538	1.01×10^{-2}	-.164	- .655	
	.0134	4.76×10^{-3}	-.189	- 1.04	
	.0052	1.17×10^{-3}	-.214	- 2.33	
	.0010	3.27×10^{-4}	-.227	- 6.0	62.1
	.0004	1.05×10^{-4}	-.236	- 15.9	62.5
	.0001	1.87×10^{-5}	-.248	- 78.3	62.96
	0.	2.34×10^{-6}	-.259	- 547.	63.4
	0.	2.14×10^{-7}	-.270	- 5125.	63.9
	0.	1.18×10^{-8}	-.280	-75355.	64.36
0.01	.7967	3.09×10^{-2}	-.019	- .007	
	.1414	1.32×10^{-2}	-.0519	- .25	
	.0595	7.79×10^{-3}	-.0884	- .8	
	.0185	3.23×10^{-3}	-.144	- 2.3	
	.0032	6.69×10^{-4}	-.199	- 6.2	
	.0012	2.75×10^{-4}	-.214	- 10.5	
	.0003	6.33×10^{-5}	-.229	- 30.8	62.22
	.0001	2.61×10^{-5}	-.236	- 65.9	62.50
	0.	6.95×10^{-5}	-.245	- 220.	62.86
	0.	4.48×10^{-6}	-.248	- 330.	62.97
	0.	7.10×10^{-7}	-.257	- 1858.	63.40
	0.	2.22×10^{-7}	-.263	- 5516.	63.64

Measurement of Velocity of Particles in Laser Beam

Photographs of the apparatus are shown in Figure 9.

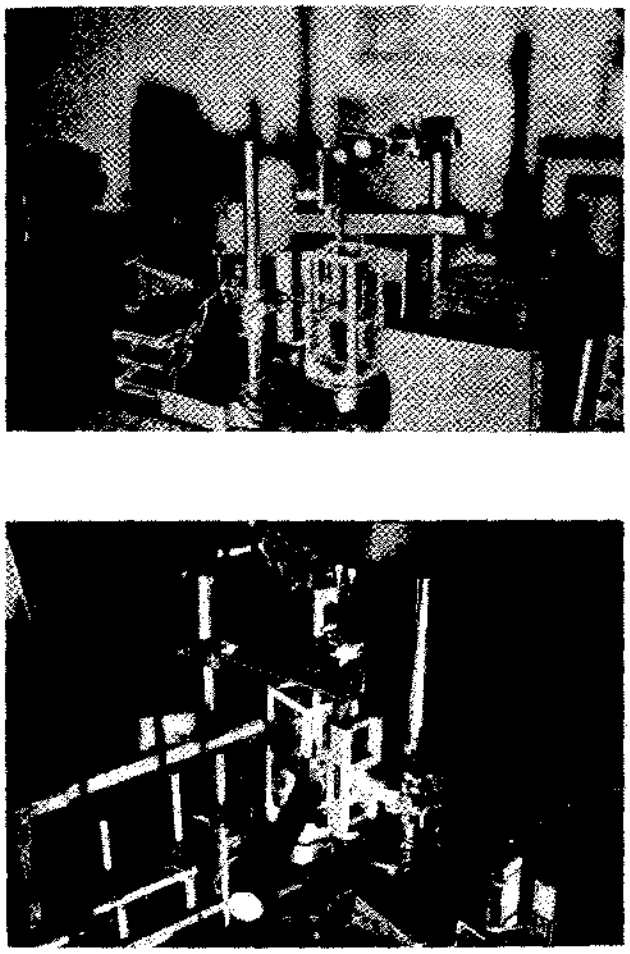

Figure 9. Two views of apparatus for measuring velocity of particles in laser beam.

Instead of relying on the presence of dust particles, a few drops of a slurry of titanium dioxide particles in brine was added to the solution. These pigment particles have a mean diameter of 0.3 micrometers, and are so small that they will move with the actual velocity of the brine without interfering with the flow.

Two methods were devised to measure the distance from a particle to the salt face. In the first method a microscope was focused on the moving particles and then on another particle that happened to be attached to the salt face. The distance through which the microscope had to be moved was measured by means of a dial gauge. The depth of field was 2 mils, and this determined the precision of this method of measurement. In the second method, the laser beam was positioned so that it penetrated only a short distance into the boundary layer. Thus, any particles illuminated must lie within the distance, which was known from a previous measurement of the laser trajectory. This method was precise to 1 mil. Furthermore, it allowed the use of a microscope objective with less magnification and greater depth of field.

Two methods were devised to measure the velocity of particles. One method was suitable for slower particles near the salt face. It was based on direct observation of the particles moving past the field of view, and comparing their time of passage with the duration of a calibrated electronic timer. By adjusting the timer to give the same duration as the particle, its time of passage could be determined. The velocity could then be calculated knowing the diameter of the field of view. This method was suitable for duration from 1 to 12 seconds. For particles with higher velocities, namely particles further out into the boundary layer, the time of passage was less than 1 second. For these particles a photomultiplier was attached to the microscope, and the light from individual particles registered on an oscilloscope. The width of the pulse of light measured the time of passage of the particle, and hence its velocity. The field of view of the photomultiplier was smaller than that of the microscope, assuring that only one particle at a time was present. This technique works well at some distance from the salt, where there are numerous particles. Close to the salt there are too few particles, and direct visual observation must be used. The apparatus is shown in Figure 12.

Velocities determined by the two methods are presented in Figures 10 to 12 for several conditions of depth and brine bulk concentration. The curve of velocity versus distance from the salt is given by the envelope of the experimental points, since particles within the field of view from the salt out to the edge of the laser illumination are all measured. The particles with the maximum velocity are the furthest out, corresponding to the edge of the laser trajectory.

The results of these measurements can be used to determine the parameters in the formula for the boundary layer velocity. Further measurements are needed, especially to reach the range of concentrations and depths of interest for solution mining.

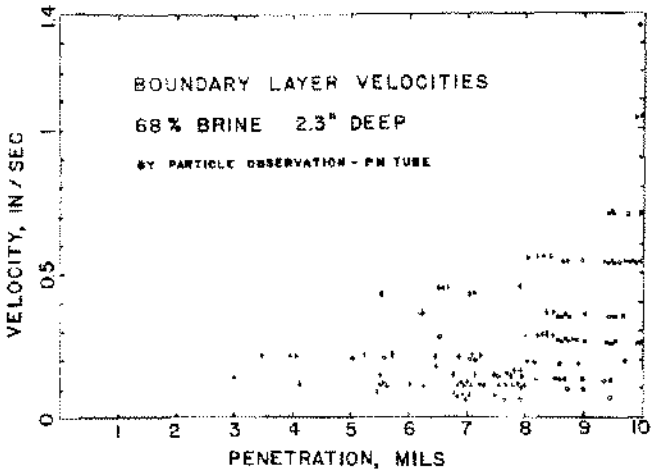

Figure 10. Boundary layer velocities, 68% brine, 2.3" deep.

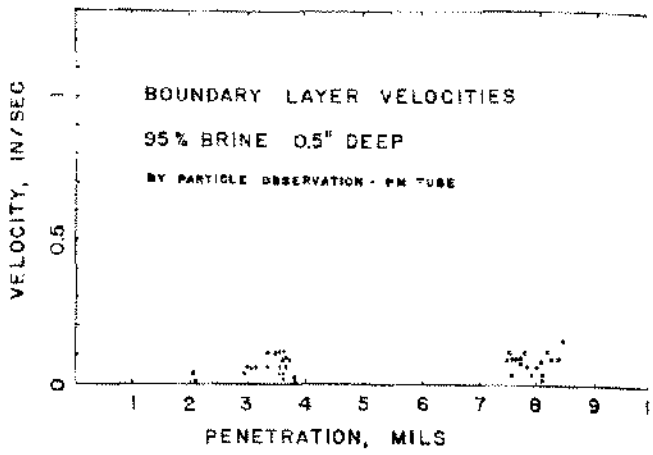

Figure 12. Boundary layer velocities, 95% brine, 0.5" deep.

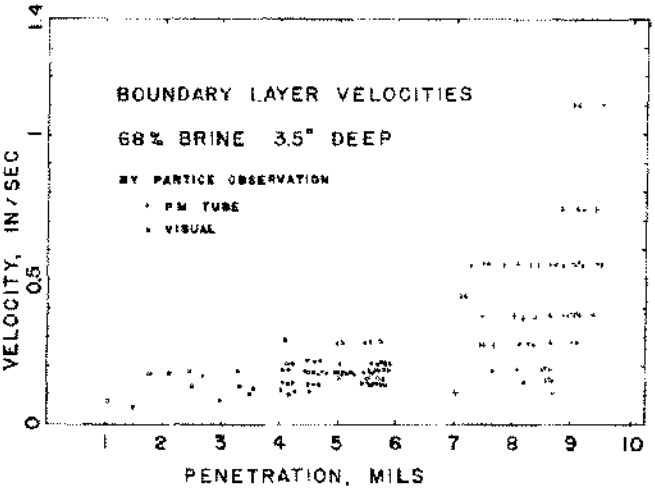

Figure 11. Boundary layer velocities, 68% brine, 3.5" deep.

Measurement of Motion of a Line of Dye

Papovich and Hummel (1967) used the method to measure the boundary layer profile for flow in a pipe, and they described preparation of a special organic chemical that forms a color in a few microseconds. Unfortunately, their dye also fades in a few milliseconds; our experiments take longer than that, because the salt boundary layer flow is slower. We decided to use the blueprint reaction to form a line of dye.

The blueprint reaction is used by Goldish, Koutsky and Adler (1965). In their method iron solution and ferricyanide solution are mixed in dim light, and the color develops rapidly on exposure to a flash tube. We used a xenon flash tube charged from a capacitor with 500 watt-sec of energy, and focused the light into a region about 1 x 4 x .1 mm in size, with the mirror arrangement of Papovich and Hummel shown in Figures 7 to 9, pages 25 to 27.

The literature (1965) indicates that only ultraviolet light is effective in producing the blueprint reaction. Quartz passes ultraviolet, while glass does not, and we found that the experiment must be done in a quartz tank rather than in glass. Furthermore, the solution itself can absorb the light before it reaches the location where it is focused. On the other hand, solid salt is transparent to ultraviolet light down to 1500 A, so we focused the light through a salt crystal cemented to the wall of the tube.

The next problem was to photograph the line of blue color produced by the light. Some still photographs were taken, but the best technique was to take a motion picture using back-lighting with a Fastax camera at 400 frames/sec. The experimental arrangement is shown in Figures 13 to 15. Several frames from these cinematographs are superimposed in Figures 16 and 17. The dark image of the dye line as it progresses down the face of the salt measures the velocity of the boundary layer. The velocity decreases linearly from the point of maximum velocity out into the bulk solution. Velocities closer to the salt can not be determined by this technique, since the boundary layer is too thin at shallow depths. At greater depths the method

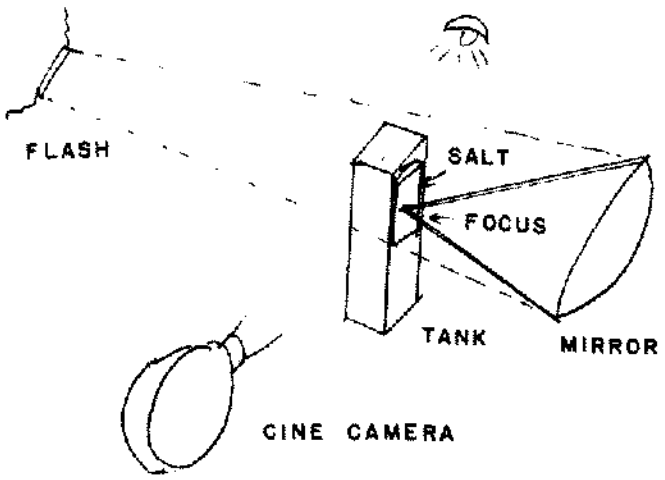

Figure 13. Apparatus for measuring boundary layer velocity profile.

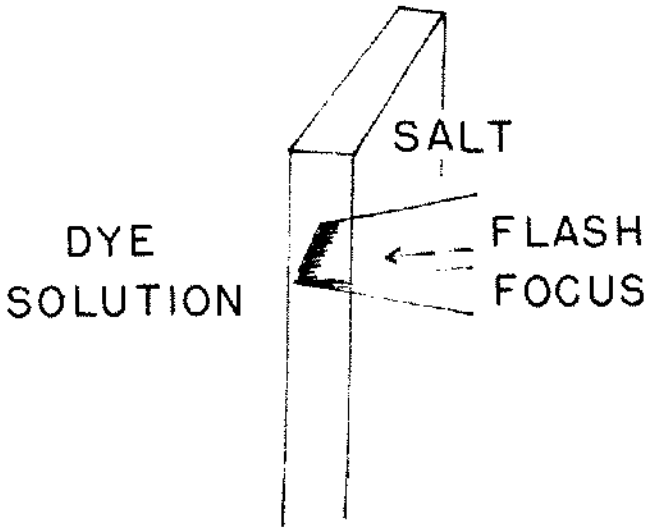

Figure 15. Geometry of dye line formation.

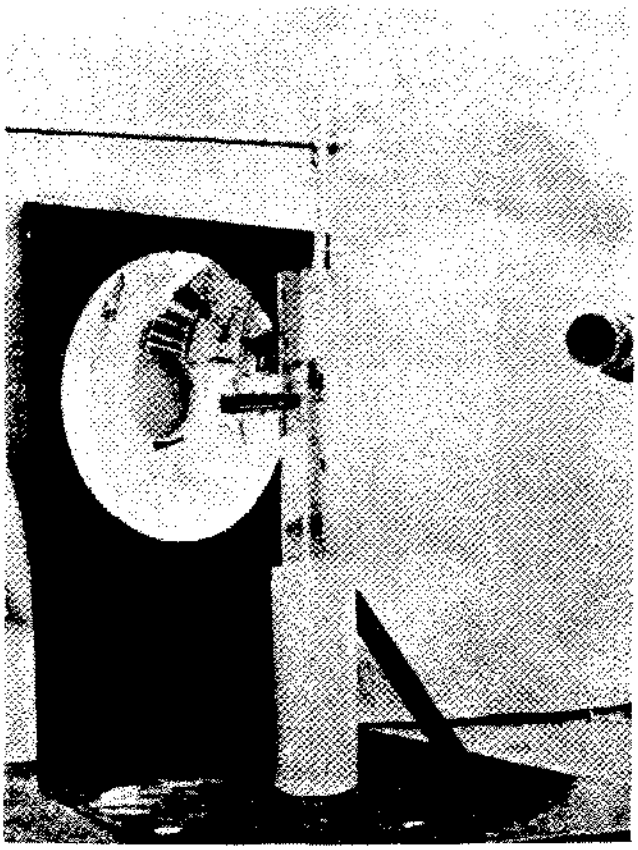

Figure 14. Apparatus for measuring boundary layer velocity profile.

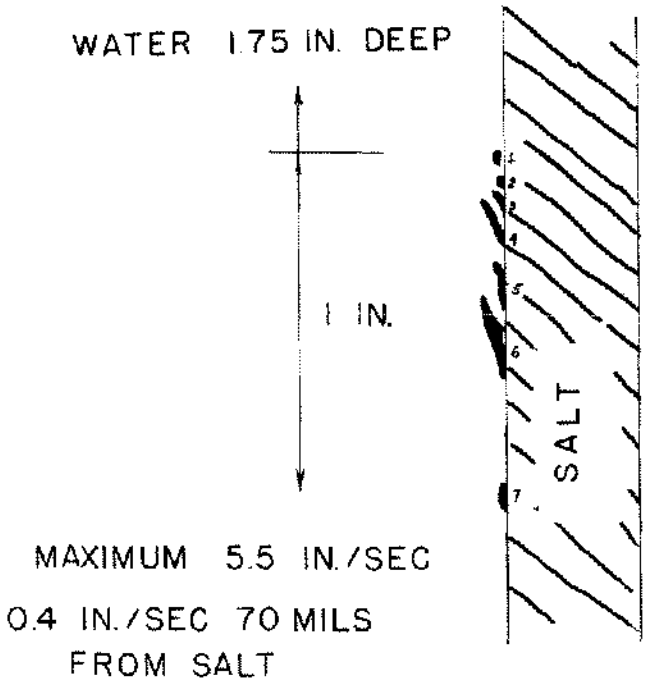

Figure 16. Images of dye lines taken from cinematographs.

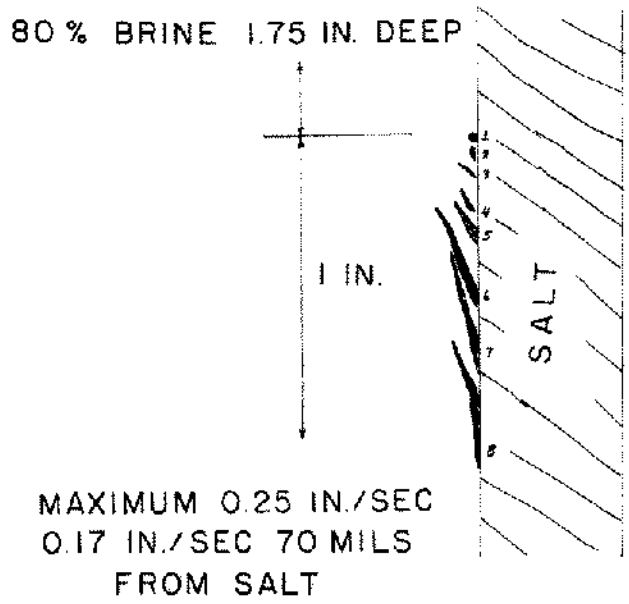

Figure 17. Images of dye lines taken from cinematographs.

could be used. The method is useful to obtain the maximum velocity, which is the most important property.

THEORETICAL MODEL FOR SOLUTION OF IMPERFECT SALT

Our present knowledge of solution of imperfect salt indicates that there are only 1 or 2 important effects, although these effects may be caused by several different types of impurities. For this reason, an approach to a model for imperfect salt can be based on a modification of the existing model for perfect salt.

An important effect occurs as the boundary layer flows over an insoluble rock layer. The salt dissolves faster below the layer than above it, so the rock layer becomes undercut. Soon the layer of concentrated brine can be seen to separate from the surface as it pours off of the bottom edge of the rock layer. Durie (1963) observed this and proposed that a new concentration boundary layer forms at the top edge of the undercut salt surface. It has the characteristics of any fresh boundary layer, being thin and having a high solution rate. Probably the formulas for a new boundary layer on a small sample of salt can be applied to predict the salt local solution rate. However, the new boundary layer should be affected somewhat by the flow of brine further out into the bulk solution. Experiments will be needed to check whether the flowing separated boundary layer can affect the new boundary layer. Further work is also needed to estimate the total quantity of fluid that is entrained by this process of boundary layers flowing off of insoluble ledges and mixing with more diluted bulk solution.

The second important effect is the development of pits or recesses. Durie attempted to apply geometric reasoning to explain these, but it appears to us that the solution rate in such a recess can also be approximated by the formula for the solution rate at the top of a salt sample, because in both cases a new boundary layer is formed. In both cases the solution rate is high because the boundary layer is thin. This would be true whether the recess is initiated by the occurrence in the salt of a bubble, crack, an insoluble grain, or a boundary between intergrown crystals. The frequency of occurrence of pits can perhaps be related to the frequency of occurrence of these imperfections. However, boundary layer flow may be augmented by an eddy in the recess. In a recent thesis, the flow pattern in such recesses was studied and found to occur as in Figure 18.

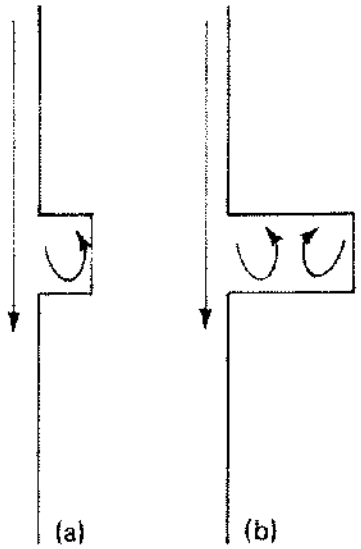

Figure 18. Circulation induced in recesses by surface flow.

In Figure (a) the recess is only deep enough for one eddy to form. Note that the induced flow moves upward at the back of the recess, against the direction of buoyancy. When the recess becomes deeper in Figure (b), two eddies form. In this case, the induced flow is in the direction favored by

buoyancy at the back of the recess. Thus, these two effects reinforce each other when the recess reaches this depth. This effect can explain the increasing solution rate as pitting develops.

Furthermore, we must recognize that a completely theoretical model of the solution process of imperfect salt is not possible at the present time. It is expected that knowledge of the behavior of imperfect salt will be augmented by observations to be made at the International Mine cavity experiment next year. Nevertheless, an approach for developing a reasonable model is available.

CAVITY GROWTH EXPERIMENT

An additional opportunity to test the cavity growth model and measure boundary layer parameters will be given by a pilot-scale experiment planned in the International Mine by the SMRI.

The effects which should be measured are: rate of regression of cavity wall and development of shape over duration of experiment by means of calipers suspended from probe holes; boundary layer concentration profile by means of capillary sampling method (this method should work in the cavity since the boundary layer will be several inches thick); velocity profiles measured by means of a hot wire anemometer of very small wire diameter; bulk solution concentrations by measuring refractive index of samples; bulk velocities as a means of checking boundary layer flow by a material balance; and concentration boundary layer thickness to account for formation of a new concentration boundary layer in recesses and under insoluble layers.

Although there are many improvements that can be made in the cavity growth model, the existing computer program provides a capability for investigating the effects of various operating conditions or cavity growth rate and production rate. It can be used for practical applications within its probable accuracy of a factor of 2.

The author thanks the SMRI and its Technical Committee for its support and guidance.

REFERENCES

Clayton, B.R., and Massye, B.S., 1967, "Flow Visualization in Water: A Review of Techniques," J. Sci. Instr. *44*, 2-11.

Durie, R.W., 1963, "The Boundary Region in the Salt Dissolution Process," Ph.D. Thesis (University of Texas), Univ. Microfilms Dissertation 64-6593.

Eckert, E.R.G., and Jackson, T.W., 1951, "Analysis of Turbulent Free-Convection Boundary Layer on a Flat Plate," NACA Report 1015.

Goldish, L.H., Koutsky, J.A., and Adler, R.J., 1965, "Tracer Introduction by Flash Photolysis," Chem. Engr. Science 20, 1011-14.

Jakob, Max, 1949, Heat Transfer, Vol. I, II, John Wiley, New York.

Kazemi, H., 1963, "Mechanism of Flow and Controlled Dissolution of Salt in Solution Mining," Ph.D. Thesis, University of Texas; Dissertation Abstracts 64-6610.

Leont'ev, A.I., and Kidryaskin, A.G., 1966, "Heat Transfer During Free Convection in Horizontal Layers," Intern. Chem. Engr., *6* (1), 126-129.

Merzkirsch, W.F., 1966, "Making Flows Visible," Int. Sci. & Technol., (October) 46-51, 118.

Papovich, A.T., and Hummel, R.T., 1967, Chem. Engr. Sci. 22, 21-25.

Schwind, R.G., and Vliet, G.C., 1965, "Observations and Interpretations of Natural Convection and Stratification in Vessels," Proceedings of the 1964 Heat Transfer and Fluid Mechanics Institute at Berkeley, Stanford Univ. Press, Stanford, p. 51-68.

Sears, G.F., 1964, Controlled Solution Mining in Massive Salt, M.S. Thesis, Univ. Texas.

Tong, J.M., 1967, "An Optical System Using Moire Patterns to Obtain Quantitative Data in a Boundary Layer," ASME paper 67-HT-3, presented at the Heat Transfer Conference, Seattle, August, 1967.

Treybal, R.E., 1968, "Mass Transfer Operations," McGraw-Hill, N.Y., 2nd Ed., p. 50.

Trump, E.N., 1947, "Mining Soluble Salines by Wells," Trans. AIME *173*, 223-9.

Wasan, D.T., Sankar, N., and Randhava, S.S., 1967, Momentum Transfer at High Mass Fluxes in Turbulent Pipe Flow, Paper presented at AIChE meeting, Salt Lake City, May 1967.

Advancement of Knowledge of Salt Dissolving by SMRI-IITRI Project

Subject	Status in 1964	Progress
Definition of Problem	Importance of Boundary Layer recognized (Durie) in small cavity experiments. Scale-up is uncertain	Agreed that B.L. has the main effect. Separated effects of imperfections. Geological variables recognized (Delwig): roof tilt, bubbles, inclusions of sand, clay, insoluble layers.
Boundary Layer Theory	Eckert and Jackson method of integrating B.L. equations was applied to salt by Durie. Analysis limited to constant bulk concentration Laminar flow profiles from forced convection assumed. Effect of wall tilt included in equation. No computer program for integrating B.L. equations was available. The computer program of Sears for cavity design uses only an empirical correlation of solution rate valid for laboratory-size samples, is expected to involve appreciable error on scale-up, and cannot predict B.L. flow, brine production and concentration.	Applied same method of integrating B.L. equations, but included turbulent profiles from forced convection, and included parameter λ to account for difference in thickness of concentration and velocity B.L. Developed computer program to integrate B.L. equations down cavity wall in presence of bulk concentration gradient, and predict B.L. flow.
Bulk Flow Behavior	Kazemi experimentally observed stratification when fresh water is fed at top of cavity. Observed peel-off of B.L. flow when stratification is encountered. Schwint and Vliet measured these effects for heat transfer.	Included mathematical analysis of these effects in cavity computer program. Can predict brine concentration and production rates.
Diffusivity of Salt	Durie used incorrect definition, involved a 25% error.	Reanalyzed data of Clack.
Forced Convection	Durie estimated that forced convection is unimportant under usual conditions.	Confirmed by calculations that forced convection is important only in initial 1 to 2 hrs of borehold growth.
Measurement of B.L. Profiles	Durie recognized that concentration B.L. is thinner than velocity B.L., and that high N_{SC} is the reason. Attempted measurements by optical projection and by simulation with wax melting were not very successful. Handicapped by imperfections in salt.	Recognized that perfect salt behaves ideally. (McCue) Preliminary measurements indicated $\lambda = 0.1$. Theoretical prediction $\lambda = .03$ based on $N_{SC} = 1000$. Developed laser bending method to measure concentration profile and flash formation of line of dye to measure velocity profile. Work is in progress.

Advancement of Knowledge of Salt Dissolving
by SMRI-IITRI Project (cont.)

Subject	Status in 1964	Progress
Comparison of Theory with Experiment	Durie found that empirical correction is needed to make B.L. prediction of solution rate agree with experiment. Results are meaningless since $\lambda = 1$ was used, and salt was imperfect in his experiments.	Found that equation relating mass transfer coefficient to shear stress in B.L. theory should have exponent of 0.52 on N_{Sc} to make theory agree with experiment for perfect salt when $\lambda = .03$. Further study of literature showed that 0.52 is more likely than value of 2/3 assumed at first.
Solution at the Roof	Durie experimentally measured solution rate. Leont'ev made an incomplete theoretical analysis.	Performed a few additional experiments, on perfect salt and rock salt.
Effects of Salt Imperfections	Observed pitting and higher solution rate under rock layer. Postulated new concentration B.L. under rock layer.	Experiments on bubble salt recognized importance of circulation in pit causing increased solution rate. In rock salt, observed that insoluble inclusions and crystal grains cause pitting to begin. Pits grow by above mechanism once formed. Postulate new concentration B.L. in pits. Observed that insoluble impurities fall off of vertical salt surfaces.
Cavity Experiment	Idea of cavity experiment at International Mine in Detroit was already proposed.	Participated with Technical Committee in design of cavity experiment to check B.L. theory and measure important parameters.